PCCP

Accepted Manuscript

ROYAL SOCIETY OF CHEMISTRY

www.rsc.org/pccp

Journal Name

ARTICLE

New insights concerning the photoswitching mechanisms of normal dithienylethenes

Received 00th January 20xx,
Accepted 00th January 20xx

DOI: 10.1039/x0xx00000x

www.rsc.org/

I. Hamdi *,[a,b] G. Buntinx,[a] A. Perrier,[c,d] O. Devos,[a] N. Jaïdane,[b] S. Delbaere,[a] A.K.Tiwari,[a] J. Dubois,[a] M. Takeshita,[e] Y. Wada,[e] and S. Aloïse *[a]

The photoswitching and competitive processes of the referent photochromic diarylethene derivatives 1,2-bis(2,4-dimethyl-5-phenyl-3-thienyl)perfluorocyclopentene (DTE) and a novel bridged analog DTE-m5 have been investigated by state-of-the-art TD-DFT calculations and ultrafast spectroscopy supported by advanced chemometrics data treatments. Focusing on DTE, the overall deactivation pathway of both antiparallel (AP) and parallel (P) conformers of the open form (OF) (1:1 in solution), have been resolved and rationalized starting from the Franck-Condon (FC) region to the ground state recovery. For the photo-excited P conformer, after ultrafast relaxation (~200 fs) toward S_1 relaxed state, an expected ISC occurred (55 ps) to produce a triplet state, ^{3}P, the latter relaxing within 2.5 µs. Concerning the AP conformer, the photocyclization reaction is reported to proceed immediately (100 fs) starting from the FC region while the relaxed singlet state is populated in parallel. For the first time, we discovered that the latter state evolves through unexpected ISC process (1 ps) giving birth to a second triplet state, ^{3}AP. For DTE-m5,by slightly constraining the molecule with the bridge, this triplet becomes reactive and participates to the formation of 10% of CF probably through an adiabatic mechanism. Concerning the photoreversion, apart from a two-step process and a photoreversion occurring probably around 6 ps, we do not succeed to give evidence for new excited state species. For the overall species at the singlet or triplet manifold, the use of advanced MCR-ALS allow us to publish specific spectral signatures. This study is therefore a new step within the comprehension of DTE photochemistry.

Introduction

In recent years much research efforts have been devoted to the development of photochromic materials i.e., systems that can be converted reversibly from one form to another upon light excitation.[1] The interest in these compounds stems from their potential applications in optoelectronics, information storage, molecular electronics, supramolecular chemistry…etc.[2] As explained in exhaustive reviews dealing with diarylethenes,[3] dithienylethenes with a perfluorocyclopentane core is one of the most efficient bistable photoswitchable molecules (thermally irreversible) regarding fatigue resistance.[4] Upon UV irradiation, dithienylethenes undergo efficient photocyclization (ϕ_{cycl}~0.2-0.5) between uncolored open form (OF) and colored closed form (CF) while switching to visible light leads to less efficient photoreversion reactions (ϕ_{rev}~0.01).[1a,2a] For photocyclization reactions based on carbone-carbone electrocyclization, the quantum yield was thought to be limited to 0.5 explained by the coexistence, in equal proportions, of two isomers having parallel (P) and anti-parallel (AP) conformations, only the latter being photoactive.[5] Overcoming this inherent limitation was the focus of various research relying on a purpose-designed synthetic approach[6] or specific excited-state reactivity.[7] Anyhow, except for few exceptions, the coexistence of the two conformers for dithienylethenes prevent a clear resolution of their individual spectral features. To discriminate between AP and P photophysics, our group has chosen the option to investigate molecules with an additional alkyl or polyether bridge between the two aryl nuclei in order to block the molecule into the photoactive AP conformation. We applied successfully such approach on 1,2-dicyano[2,n]metacyclophanene[8] or inverse dithyenylethenes.[9]
This last decade, considering studies in solution, both photocyclization [8,10] and photoreversion mechanisms [11] have been investigated intensively through a combination of time-resolved spectroscopies and calculations. The photoswitching mechanisms into the crystalline phase have also been investigated.[12] It is worth to remind that photocylization is an ultrafast process ranging from hundreds femtosecond to several picosecond[12a,b] occuring within the S_1 state maniflod from the Franck-Condon (FC) region through a

[a] Univ.Lille, CNRS, UMR 8516, LASIR, Laboratoire de Spectrochimie Infrarouge et Raman, F59 000 Lille, France.
[b] Laboratoire de Spectroscopie Atomique, Moléculaire et Applications– LSAMA, Université de Tunis El Manar, 1060 Tunis, Tunisia.
[c] Université Paris Diderot, Sorbonne Paris Cité, 5 rue Thomas Mann, 75205 Paris Cedex 13, France.
[d] Chimie Paris Tech, PSL Research University, CNRS, Institut de Recherche de Chimie Paris (IRCP), F-75005 Paris, France.
[e] Department of Chemistry and Applied Chemistry, Faculty of Science and Engineering, Saga University, Honjo 1, Saga 840-8502, Japan.

* Corresponding authors: stephane.aloise@univ-lille1.fr
Electronic Supplementary Information (ESI) available: See DOI: 10.1039/x0xx00000x

conical intersection (CI) well identified by advanced CASSCF/CASPT2 calculations.[13] The exact mechanism, either direct (FC→CI) or requiring an initial relaxation within relaxed S_1 state (FC→S_1(rel)→CI), being always a delicate question.[14] Concerning photoreversion, the low value of the quantum yield is explained by the presence of high energy barrier within excited state pathway before reactive topologic point.[12c,15] Additionally, novel photocyclization pathways have been found through excitation of high excited states[7] or triplet excited states. By the way, during these last years, several groups have paid more and more attention on the role of the low-lying triplet excited state populated either by sensitization[16] or intersystem crossing (ISC) enhanced by appropriate dyad substituent.[16a,17] Furthermore, the special involments of triplet species within photooxidation process of dithienylethenes have been reported recently.[4]

Among normal dithienylethenes, 1,2-bis(2,4-dimethyl-5-phenyl-3-thienyl) perfluorocyclopentene called later DTE (see Scheme 1) recovers special importance due to the excellent fatigue resistance reported with more than 850 switching cycles.[4] This is the reason why this molecule is commercially available by several companies since decades and consequently purchased by worldwide [8,10] groups who need a molecular switch to get a proof of principal (patents) dealing with applicative topics like semiconductor applications,[18] optical memories,[19] and smart ink,[20] as few examples. Focusing on spectroscopic techniques, DTE has been used in papers dealing with sequential two-photon cycloreversion technique,[21] time-resolved Raman spectroscopy,[10a] 2D femtosecond stimulated Raman technique,[22] photochromism of single crystals[12a] and femtosecond electron diffraction.[12b] Clearly, DTE molecule is extensively used by a broad spectroscopists community and thorough rationalization of the photoswitching mechanisms is highly desired taking into consideration that several competitive pathways can co-exist.

As a consequence, recent papers on DTE have been published. In 2014, DTE photocyclization in solution was studied by Pontecorvo et al[10a] with both femtosecond transient absorption and Raman spectroscopies to unravel AP and P photochemistry. Both conformers co-exist in equal proportion as proved by ^{1}H-NMR measurements AP:P ratio being 48:52.[23] They reported that the electrocyclization reaction takes place in ~ 300fs while a triplet state coming from the P conformer was populated according to ISC process within ~23 ps; no AP triplet state was detected by this group. Note that they did not investigate the decay mechanism of DTE triplet state referring to the decay of another representative photochromic diaryléthène; 1,2-bis(2-methyl-3-benzothienyl) perfluorocyclopentene(BT) instead.[10b] In parallel, the cycloreversion dynamics for DTE molecule has been studied by Ward *et.al* [21a] using sequential two-photons excitation (pump-repump-probe) ultrafast spectroscopy. Transient data have been interpreted in terms of ultrafast relaxation from FC region (~100 fs) to relaxed excited state S_1 overpassing a barrier (~3 ps) and final internal conversion (IC) to the ground state manifold (~9 ps). Note that no spectral signature distinguishing FC from relax states has been proposed.

In the present paper, we aim to review both photoinduced ring-opening and ring-closing process using the combination of femtosecond and nanosecond absorption spectroscopy apparatus supported with time-dependent density functional theory (TD-DFT) calculations. We are interested to determine the individual spectral signature of any electronic excited states regardless it is populated efficiently or not. This challenging task will be undertaken with the aid of multivariate curve resolution methods (MCR-ALS) which is able to extract hidden spectral signature of intermediate states.[24] Furthermore, in this study, we paid more attention to the triplet states photophysics. To do so, we continue our approach investigating a neighboring analog called DTE-m5 with an additional polyether chain (see Scheme 1) which induces a constraint on the DTE core. At first glance, this molecule was thought to freeze the molecule into the parallel conformation following our strategy we initiated for inversed diarylethene (bis(3,5-dimethyl-2-thienyl)-perfluorocyclopentene).[9] As we will see, this point will be crucial to open a new photocyclization pathway in the microsecond time-scale.

Scheme 1:

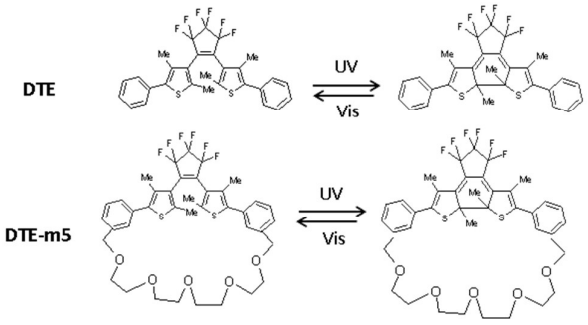

EXPERIMENTAL AND THEORITICAL METHODS

Stationnary techniques.

The dithienylethene DTE is a commercial compound (sigma Aldrich) and the bridged DTE-m5 was synthesized by Takeshita *et al* [25]and the preparation is detailed in supporting information (Document S.0). Chloroform ($CHCl_3$) solvent (spectroscopic grade, Sigma-Aldrich) was used as received. The stationary absorption spectra were measured with CARY 100bio absorption spectrometer. ^{1}H-NMR spectra in $CDCl_3$ were recorded on Bruker Avance-300 (300 MHz). The photocyclization and photoreversion yields have already been published for DTE[23] and were determined in this work for DTE-m5 according to usual procedure.[25]

Transient absorption techniques.

Our nanosecond transient absorption spectroscopy setup has been described elsewhere.[26] Briefly, a third harmonic pulse (355 nm) of a Nd:YAG laser with ca. 1mJ output power and 5 ns pulse width was used as excitation light and a pulsed Xe lamp was utilized as probe light. Transient absorption spectra were obtained from the transient absorption decays recorded at various wavelengths by sampling the absorbance changes for different given delay-times. The triplet yields ϕ_T of DTE and DTE-m5 were determined by energy transfer to β-carotene compared to the results obtained with benzophenone (Bp) using 320 nm excitation wavelength. For this experiment, benzophenone and DTE solutions were optically matched at 320 nm. The following equation for triplet yields was used.[27]

$$\phi_T = \frac{\Delta A_\infty^{DTE}}{\Delta A_\infty^{Bp}} \frac{K_{obs}^{DTE}}{K_{obs}^{DTE} - K_0^{DTE}} \frac{K_{obs}^{Bp} - K_0^{Bp}}{K_{obs}^{Bp}} \phi_{Bp} \qquad (1)$$

Where, ΔA_∞^{DTE} and ΔA_∞^{Bp} designate the plateau absorbance for DTE and benzophenone, K_{obs} is the pseudo-first-order rate constant for the growth of the β-carotene triplet and K_0 is the rate constant for the decay of the triplet donor (DTE, DTE-m5 or benzophenone), ϕ_{Bp} is the triplet yield of benzophenone.

Femtosecond time-resolved experiments were performed using a pump-probe spectrometer[28] based on Ti:sapphire laser system (Coherent Mira-900-D oscillator and Libra-S regenerative amplifier) delivering 800 nm, 1 mJ and 90 fs pulses with a repetition rate of 1 kHz. The pump pulses adjusted @ 320 nm were generated by

frequency quadrupling the output of a Quantronix Palitra OPA pumped at 800 nm and the energy at the sample was about 2 µJ ($0.2\ \mathrm{mJ\ cm^{-2}}$). Note that, we choose to excite the molecule far from the maximum of absorption localized near 270 nm to avoid short-time signal coming from solvent. The probe pulses were obtained by focusing 1 µJ, 800 nm pulses into a 1 mm CaF2 plate to generate a white light continuum. The pump-probe polarization configuration was set at the magic angle (54.7°). Transient absorbance was obtained by comparing signal and reference spectra with and without pump pulses for different delay times. The delay time between the pump and probe was varied up to 0.5 ns using an optical delay line. Sample solutions ($\sim 10^{-3}\ \mathrm{mol\ dm^{-3}}$, OD=1 at the pump wavelength) were circulated in a cell equipped with 200 µm thick CaF_2 entrance window and having 2 mm optical path length. The sample solution was circulated during measurements and was irradiated by CW Xe lamp visible light to prevent the formation of CF. In this configuration, for 320 nm excitation, the instrumental response function determined by fitting the Stimulated Raman transient pic of acetonitrile was determined to be 180 fs. All the transient spectra presented in this paper are GVD corrected according to the typical extrapolation method[29] (the temporal chirp over the white-light 350-800 nm range was about 400 fs). The characteristic times deduced from kinetics are obtained by fitting the data with the result of a multiexponential function convolved with a Gaussian pulse mimicking the pump-probe cross-correlation function (FWHM at 180 fs).

Theoretical Calculations

All the calculations have been performed by using the Gaussian 09 package.[30] The density functional theory (DFT) and time dependent DFT (TD-DFT) calculations to model ground-state (GS) and excited-state (ES) properties, respectively. In the course of the geometry optimization, we used the ωB97XD range-separated hybrid (RSH) functional combined with the 6-31G (d) atomic basis set. Contrary to the conventional hybrid functional, RSH are known to avoid inconsistencies for ES geometries.[9] For all the optimized structures, vibrational frequencies were computed to ensure that the geometries correspond to true minima of the potential energy surfaces. All the geometry optimizations have been carried out in $CHCl_3$, applying the Polarizable Continuum Model (PCM)[31] to quantify the impact of the environment. The GS and ES geometry optimizations have been carried out in the equilibrium limit using the linear-response (LR) PCM scheme. For the GS, the transition state (TS) searched for both DTE and DTE-m5 molecules have been performed using the Synchronous Transit-Guided Quasi-Newton (QST3) method.[32] For the lowest triplet state exploration (T_1), we have used the unrestricted formalism and systematically checked the spin-contamination.

The optical properties have been determined using vertical TD-DFT calculations computed with the LR-PCM scheme in its non-equilibrium limit. We have compared the results obtained with two different computational strategies namely the ωB97XD/6-31G(d) method that is used in the course of geometry optimizations and the CAM-B3LYP/ 6-311+G (2d,p) methodology. The latter scheme is actually known to reproduce accurately the observed absorption wavelengths of dithienylethenes.[14] For the CF isomer, we have obtained a maximum absorbance wavelength of 502 nm with ωB97XD/6-31G(d) and 526 nm with CAM-B3LYP/ 6-311+G (2d,p) which respectively leads to an error of +0.33 eV and +0.22 eV if we compare with experimental measurements (575 nm, see Table 1). We have thus decided to rely on the CAM-B3LYP/ 6-311+G (2d,p) strategy to determine the spectroscopic parameters.

RESULTS AND DISCUSSION

Our goal is to achieve a deep understanding of the photophysics of DTE and bridged analog DTE-m5 with the special challenge to distinguish between the contributions coming from the P and AP conformers as we did the for 1,2-dicyano[2,n]metacyclophanene[8] and inverse pentafluoro-dithienylethene.[9,33] As a matter of fact, we track some new pathways for the photocyclization with a special interest for the triplet state suggested by Herder et al.[4] To do so, we first assess the exact proportion of P and AP conformers, for both molecules using ^{1}H-NMR measurements. Concerning respective optical properties, absorption spectra were analyzed by the aid of TD-DFT calculations. Finally, the excited states dynamics were investigated using distinct ultrafast spectroscopy setups for probing singlet (femtosecond laser setup) and triplet photophysics (nanosecond laser-flash photolysis). For the first time, we used multivariate curve resolution alternating least squares (MCR-ALS) method to obtain the pure spectrum for the triplet and singlet species of both AP and P conformers.

Basic properties of DTE series

First of all, it is worth to remind that the P:AP ratio of DTE has been unambiguously determined based on ^{1}H-NMR measurements to 52:48 at ambient temperature (in $CDCl_3$)[23] in reasonable accordance with the Boltzmann populations (67:33), calculated from the Gibbs free energies obtained at the PCM-ωB97XD/6-31G(d) level. For DTE-m5, similar ^{1}H-NMR measurements give a 60:40 ratio (see Figure S1). One can note that the decrease in photocyclization yield from 0.46 to 0.36 (see Table 1) parallels the decrease of AP population from 48 to 40%. Clearly, we failed to reduce significantly the proportion of AP conformer however studying DTE-m5 has still an interest as we will see later. Anyhow, it is worth to investigate the vertical excitations responsible for OF spectra considering the existence of AP/P conformers as we did for inverse dithenylethenes.[14] Note that previous TD-DFT calculations have been done by Morrison et al.,[12a] with the moderate B3LYP/6-31G (d) level of calculation focusing on the AP conformer, the only one present in single crystal phase. As displayed in Figure 1, it is important to highlight that theoretical absorption spectra are merely similar with maximum at 266nm and 267nm for AP and P respectively. For both conformers, this band arises from $\pi - \pi^*$electronic excitations where the involved occupied and unoccupied π orbitals are localized on the phenyl-thienyl lateral chains (see, in SI, Tables S.18 and S.20 for description of the electronic excitations and Figures S19 and S.21 for a representation of the molecular orbitals).

After adding the polyether chain in DTE-m5, the maximum of absorption band shifted slightly compared to DTE (16 nm experimental shift). As a matter of fact, TD-DFT calculations show that there is no modification in the FC states as compared to DTE for the P conformer. On the opposite, for the AP conformer, there is an inversion of the two quasi degenerated S_2 and S_3 states and a blue shift of the $S_0 \rightarrow S_4$ electronic transition. This modification arises from the constraint imposed by the polyether chain which increases the distance between the two reactive carbon atoms, 3.78 Å for DTE and 3.89 Å for DTE-m5 (Tables S.15 and S.17). This structural modification has an impact on the electronic properties as shown by the representation of the first unoccupied molecular orbitals in Figure S19, which should lead to a modification of the AP conformer photoreactivity. For both DTE and DTE-m5, it is worth to

note that for the AP isomers, due to the multi-state nature of the low-lying singlet excited states along the photocyclisation pathway[13], it was not possible to investigate the topology of the S_1 excited state with TD-DFT.

Table 1. Wavelength of maximum absorbance for OF and CF (in Chloroform) compared with PCM-TDDFT calculation for DTE and DTE-m5. Experimental quantum yields are displayed.

		λ_{abs}^{max}(nm)		Quantum yields		
		OF	CF	Cyclization	Reversion	Triplet
DTE	Exp	273	575	0.46	0.015	0.4
	theo	266 (AP) 267 (P)	526			
DTE-m5	Exp	289	580	0.36	0.015	0.55
	theo	271 (AP) 278 (P)	513			

The analysis of CF spectra is straightforward and strictly similar for both molecules. For DTE the visible band of CF peaking at 575 nm is assigned to $S_0 \rightarrow S_1$ excitation while the UV band peaking at ~~xxx~~ 373 nm is related to the S_2 state. For both compounds, these two bands arise from $\pi - \pi^*$electronic excitations as shown by TD-DFT and orbital analysis presented in Supporting Information (Figure S19-S21). As a matter of fact, due to inefficient constraint on CF geometry, we do not expect a change for the photophysics for both molecules. By the way, photoreversion yields (0.015) are strictly similar for both molecules.

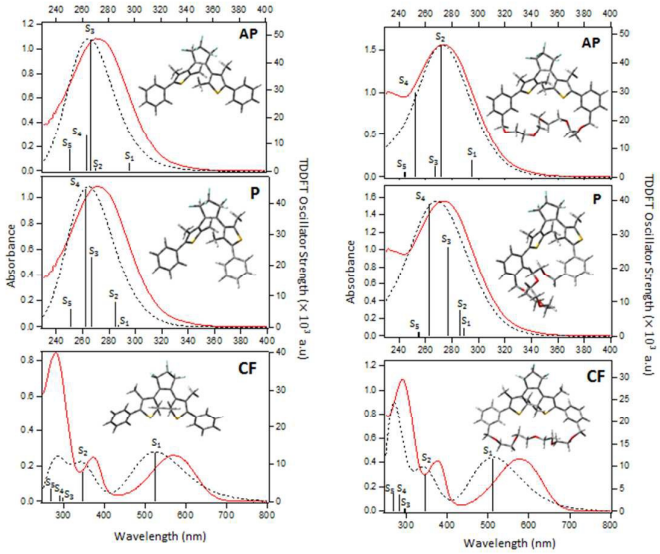

Figure 1. Comparison of experimental absorption spectra (red line) of DTE (Left) and DTE-m5 (Right) with PCM($CHCl_3$)-TD-CAM-B3LYP/6-311+G(2d,p) calculations for AP, P and CF (dashed line). Spectra are obtained after convoluting by 0.33 eV FWHM Gaussian function.

Photoreactivity of triplet species (microsecond regime).

Apart from one spectrum reported by Pontecorvo et *al.*,[10a] a careful investigation of the photophysics of DTE in the microsecond regime has never been reported. Although the distinct vibrational signatures of AP and P conformers have been obtained,[10a] the electronic spectra of the various excited states are still missing. The transient absorption spectra of DTE were recorded in the 350-700 nm spectral range, within the 0.2-180 µs time window after laser excitation at 355 nm and are shown in Figure 2. At 0.2 µs, the transient signal is almost similar to the CF absorption spectra (two absorption bands located near 350 and 570 nm) with a very weak additional transient band peaking probably near 450 nm and decaying within two stages. First within the 0.2-6 µs time window, spectral evolution shows a subsequent decrease in the 440-450 nm range while during the 9-180 µs time domain the decrease is so weak that it is difficult to notice any characteristic band. Finally, after 180 µs, all the decaying processes are over letting appear the CF spectra (see photostationnary state (PSS) spectra; black dashed curved). Note that strictly similar transient data are obtained for DTE-m5 (see Figure S2 in SI). Decay profiles for selected wavelengths are presented in Figure 3. As seen in Figure 3a, the transient kinetics (blue curve at 440 nm) is well-fitted with a biexponential function with decay times of 2.5 (80%) and 25 µs (20%) (data reported in Table 2). After addition of oxygen in the solution, both the decays are totally quenched, which suggest that both transient species are probably triplet states that we denoted by T_1 and T_2. Unlike DTE molecule, the bridged DTE-m5 (Figure 3b) molecule kinetics was fitted by a tri-exponential function with decay times of 1.7 (35%), 11.5 (55%) and 43µs (10%). Surprisingly, the three decay times were totally quenched by oxygen but the hypothesis of three triplet species is hard to believe. So, the nature of this additional species denoted species X as well as T_1 and T_2 has to be confirmed. To do so, we undertook a Stern-Volmer analysis using 2,5-Dimethyl-2,4-hexadiene as a quencher. As seen in Figure 4a and 4b, for the two molecules, the observed decay rate constants k_1^{exp} (species T_1) and k_2^{exp} (species T_2) at 440 nm depend linearly on the quencher concentration according to Stern-Volmer equation:

$$k_n^{exp} = k_n^0 + k_n^Q [Q] \quad n = 1,2 \qquad (2)$$

Both intrinsic decay k_n^0 and quenching constant k_n^Q values (n = 1, 2) are given in Table 2. For both molecules, significant quenching effects induced by the diene give the final evidence for the triplet nature of both transient T_1 and T_2 species. Reversely, the species X is not quenched by the diene and observed only for DTE-m5, which is probably a conformational process induced by the polyether chain. Note that we exclude the possible photodegradation of the sample as proved by unchanged stationary OF spectra after successive quencher addition (see Figure S5). The non-dependence on oxygen adduct is still not clear, but the statistical weight of X being around 10% we will neglect this contribution in the following. By the way, as seen in Table 2, it is worth to notice that the quenching rate of T_1 (k_1^Q) is one order of magnitude higher as compare to the T_2 one (k_2^Q), such a difference being in accordance with the distinct molecular conformations of the AP and P triplet conformers. Geometries of triplet species will be commented later with TD-DFT support. However at this point, we are still not able to assign definitively both transient species T_1 and T_2 to the conformer triplet ^{3}AP and ^{3}P. Note that we excluded the possible existence of ^{3}CF because we never detected such species after ^{1}CF visible excitation (see below). As a matter of fact, photoreactivity of such triplets toward CF species can help for such unambiguous assignment.

As recently reported by several groups, the cyclization reaction of dithienylethene can take place at the triplet manifold either based on intermolecular energy transfer in dyad system[16a] or triplet sensitization.[16c] Specifically for DTE, Pontecorvo et *al*,[10a] have reported that the triplet production is nascent from P conformer. To the best of our knowledge, we are the first group to report the two triplet states. We have investigated their photoreactivity paying attention to the CF plateau variation at 580 nm upon quencher addition (few percents of photocyclization reaction can be expected to come from the triplet manifold). First, comparing the oxygen effect for both molecules (CF plateau at 580 nm in Figure 3a and

3b), one can immediately notice that the final quantity is not changing for DTE whereas, a 10% diminution is reported for DTE-m5. This result gives evidence for a small part of the CF population formed by ^{3}AP as precursor but we still need to assign the latter one to either the T_1 or the T_2 states. Then, the Stern-Volmer dependency on DTE-m5 CF signal upon quencher addition is analyzed: the intensity of the long time absorbance plateau at 580 nm in presence of quencher (ΔA_∞^Q) is expected to vary according to equation 3:

$$\frac{\Delta A_\infty^0}{\Delta A_\infty^0 - \Delta A_\infty^Q} \approx 1 + \frac{k_n^0}{k_n^Q}\frac{1}{[Q]} \qquad (3)$$

Where, ΔA_∞^0 is the final absorbance plateau at 580 nm in the absence of quencher (this equation has been established according to some approximations presented in supporting information). On the one hand, as seen in Figure 4c, a linear correlation is indeed observed according to equation 3 with a slope equal to 0.038. On the other hand the two ratios k_n^0/k_n^Q computed from the quenching data (equation 1) of T_1 and T_2 (see Table 2) are respectively 0.014 and 0.034 which allows assigning T_2 to ^{3}AP. At the present, the assignment is not ambiguous anymore: T_2 species is assigned as the only triplet conformer able to cyclized, i.e., ^{3}AP and logically T_1 have to be assign as ^{3}P. Furthermore, unlike DTE, we reported here for DTE-m5, a new photocyclization pathway via, the triplet state comparatively to the expected classical singlet pathway. The additional molecular constraint due to the polyether chain must be probably responsible for such effect but we will discuss this point latter. Finally, to appreciate in better way the singularities of both the triplets, we presented in Figure 2b MCR-ALS decomposition (see Figures S11 and S12) of transient data to distinguish ^{3}P and ^{3}AP spectral signatures. The pure spectrum of ^{3}P is intense and peaking near 460 nm whereas the ^{3}AP spectrum is weaker and wider without a noticeable maximum.

To rationalize the new photocyclization pathway observed only for DTE-m5 via the triplet state (^{3}AP →CF), a TD-DFT computational study has been performed for both molecules with optimized ^{3}AP structures. The results are displayed in an energy diagram in Figure 5, comparing the ground state AP(S_0) and the lowest triplet states ^{3}AP energy versus the CC distance between reactive carbons R_{CC}. As immediately seen on this figure, a drastic structure effect is noticed comparing the ΔR_{CC} difference between the ^{3}AP and AP (S_0) minima: the moderate decrease of 0.11 Å for DTE contrasts with the substantial decrease of 0.73 Å for DTE-m5 (see Figure 5). As an evidence, rationalization of such effect is the keypoint of this study. Clearly, this structure effect is not due to a change of MO. The electronic structure of ^{3}AP is not modified by the additional bridge as shown by the analysis of the singly occupied molecular orbitals and spin density (see, Figure S18 and S19). Reversely, close inspection of DFT structures is much more instructive.

Indeed, one can first notice a stretching of the central double bond of ^{3}AP as compared to the AP (S_0) structure. For DTE (DTE-m5) this distance is 1.346 Å (1.347 Å) for AP (S_0) and 1.487 Å (1.478 Å) for ^{3}AP. The double bond character of the central C-C bond is thus lost for the AP triplet minimum as already shown by Indelli and coworkers[16a] for diarylethene models, namely 1,2-bis(3-thienyl)ethene compound (CASSCF calculations) and 1,2-bis(2-methylbenzothiophene-3-yl) maleide molecule (DFT calculations). As a consequence, the ^{3}AP geometry of DTE-m5 has to face two constraints, (i) the stretching of the C=C central bond and (ii) the additional constraint imposed by the polyether bridge, which brings the two phenyl-thienyl chains closer. The competition between these two constraints thus leads to a compression of the DTE core and to a decrease of the distance between the two reactive carbon atoms which rationalize the structure effect reported above. Finally, still closer inspection of the triplet and singlet potential energy surfaces (PES) shows that this structural modification may have a strong impact on the cyclization reaction. For ^{3}AP, the plateau leading to the transition state TS_1 becomes less wide for DTE-m5 (0.73Å) as compared to DTE (1.24 Å) and thus the system should more efficiently reach the transition state region which finally brought a robust explanation for the second pathway opened by the structural modification.

Table 2. Lifetimes deduced from multiexponentiel fitting of transient kinetics obtained from the laser-flash photolysis experiment (the relative contributions is given into parenthesis) for DTE and DTE-m5. Quenching rate constants of T_1, T_2 and CF species are indicated (see text).

	Lifetimes (µs)			Quenching rate ($10^8 M^{-1}s^{-1}$)		
	τ_1	τ_2	τ_3	k_1^Q	k_2^Q	k_{CF}^0
DTE	2.55(3) (80%)	25.5(4) (20%)	… 22.23(1)	0.10(4)	….	
DTE-m5	1.65(4) (35%)	11.6(3) (45%)	43(1) (20%)	1.17(6)	3.92(1)	0.036(7)

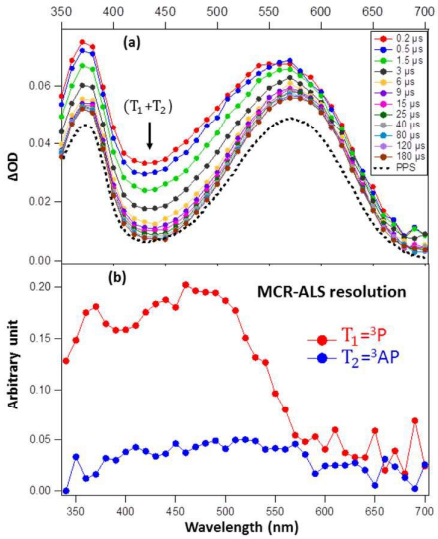

Figure 2. (a) Sub-picosecond time-resolved spectra of DTE in chloroform using 355 nm excitation. (b) Spectra of triplet state AP and P conformers, respectively obtained by MCR-ALS approach.

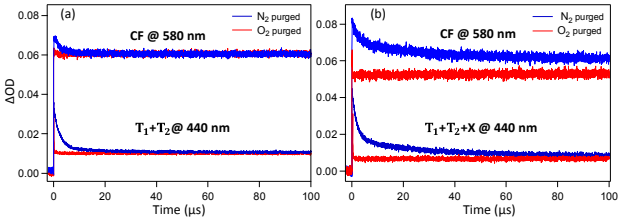

Figure 3. Time profiles of the transient absorbance of DTE (a) and DTE-m5 (b) in chloroform at 440 nm and 580 nm respectively. Solutions were initially purged with N_2 gas (blue line) or O_2 gas (red line).

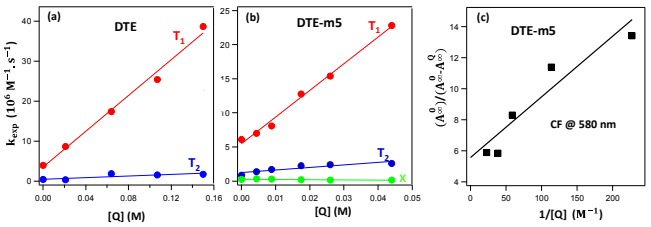

Figure 4. Stern-Volmer plots concerning DTE (a) and DTE-m5 (b) respectively: experimental decay k_{exp} of two triplet states obtained from kinetics at 440 nm wavelength function of quencher concentration [Q]. (c) Calculated ratio (eq3) obtained from long time plateau absorbance of CF at 580 nm function of the inverse of quencher concentration.

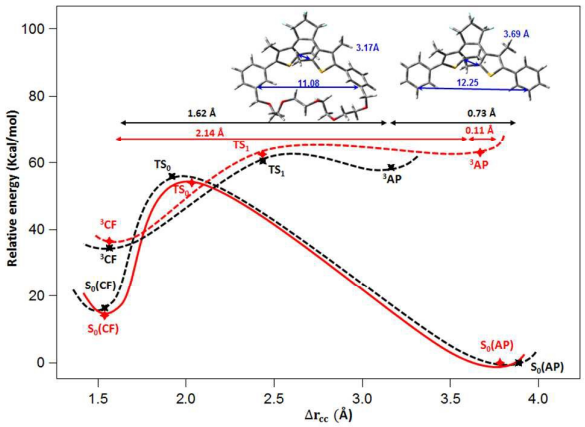

Figure 5. Topologic points within S_0 and T_1 manifolds calculated at the PCM(CHCl3)-uCAM-B3LYP/6-311+G(2d,p) level for the geometries optimized with PCM(CHCl3)-ωB97XD/6-31G(d). The lines are schematic representation of the potential energy profiles for DTE (red line) and DTE-m5 (black line). The variation of the main geometrical parameters along the reaction coordinate can be found in the SI.

Reconsidering the photocyclization process (femtosecond regime).

The discovery of both ^{3}AP and ^{3}P implies to review the post-excitation mechanism of the OF published in the past with a special focus on the two expected ISC processes responsible for the formation of these two triplets. Despite of the difference observed in microsecond regime between DTE and DTE-m5, the behavior of both molecules are similar in femtosecond regime. In the following, we present only the femtosecond results obtained for DTE. The major results obtained for DTE-m5 molecule are described in supporting information (see Figure S.6).

Transient absorption spectra recorded for DTE (in chloroform) following 320 nm laser excitation within four time windows (0-0.22, 0.28-0.90, 1-3 and 5-300 ps) are shown as parts a, b, c and d, respectively in Figure 6 (350-700 nm spectral range). Global fitting of transient signals with four-exponential functions convoluted with a Gaussian (see Figure S7 and Figure S8) and final characteristic times are gathered together in Table 3. In the first panel, just after laser excitation of the OF (uncolored solution), one noticed the rise of a major excited state absorption (ESA) with two distinguishable maxima peaking at 360 nm and 410 nm. One has to take into consideration that both AP and P are in similar proportion (~50%) and possess identical absorption spectra (see TD-DFT results above) which implies that both conformers have to contribute to this native ESA. By anticipation, we assign the 360 nm feature to the FC singlet state absorption of the AP conformer i.e., $S_1^{FC}(AP)$, while the 410 nm shoulder is related to the P conformer, i.e., $S_1^{FC}(P)$. The analysis of the 0.28-0.9 ps temporal window is characterized by two important spectral features: i) the ultrafast decrease of $S_1^{FC}(AP)$ ESA band at 360 nm concomitant with the rise of a new ESA visible band within 500-700 nm which coincide with the typical CF absorption (see black dashed curve); ii) the $S_1^{FC}(P)$ is barely constant. Both observations are consistent with an ultrafast ring closing reaction proceeding directly from the FC region while the P conformer has not initiated its own deactivation process (constant signal). As seen in Table 3, the characteristic time for this photocyclization process is about 100 fs which is lower as compare to the 300 fs, obtained by Pontecorvo et *al*.[10a] In the past, such short lifetime have been already reported for bridged diarylethene (120 fs),[8] for inverse dithienylethene (100fs)[9] and for a photochromic diaryléthène derivatives,1,2-bis(2-methyl-3-benzothienyl)perfluorocyclopentene (BT), in nonpolar alkane solution (450 fs).[10b] Note that earlier publications dealing with diarylethene, reported photocyclizations longer than 1 ps which is probably overestimated.[34] With anticipation, apart the CF ESA, it is worth to consider that the rise of the new ESA band contains also a contribution from the expected relaxed singlet state $S_1^{rel}(AP)$. Indeed such singlet state being the precursor of ^{3}AP according to ISC process, it might appear during FC state relaxation; in other word, we propose that photocyclization and vibrational relaxation into relaxed state proceed along two parallel (and competitive) pathways. The overall photocyclization process is presented in Figure 8. For times longer than 1 ps, one observes merely distinct decaying processes. Indeed, on the third panel (until 3 ps) a short decrease of ESA signal around 480 nm is noticed while on the fourth panel (5-300 ps) this signal corresponding to the maximum of triplet ESA is invariant during the double exponential decay of ESA bands near 425 and 560 nm. Logically, reminding that the ISC process will be the terminal one during the picosecond regime, we assigned the shortest decay with 200 fs characteristic time to be the IC relaxation process $S_1^{FC}(P) \rightarrow S_1^{rel}(P)$ while 1 ps and 55 ps times were assigned to the ISC processes giving birth to the two triplet states i.e., ^{3}P and ^{3}AP as shown in Figure 8. Due to spectral and temporal overlaps, the unambiguous distinction between those processes is not straightforward but referring to previous nanosecond laser-flash photolysis experiments, the main signal can be assigned to the non-reactive conformer. By consequence, we decided to assign the 55 ps time (in chloroform) to $S_1^{rel}(P) \rightarrow {}^3P$ in accordance with the 23 ps (in cyclohexane solvent) reported by Pontecorvo et al. [10a] While the 1 ps lifetime has to be connected to with the $S_1^{rel}(AP) \rightarrow {}^3AP$ process.

Table 3. Characteristic times deduced from the global fitting method applied to femtosecond transient absorption data for DTE and DTE-m5 open and close forms excitations respectively.

	Open form excitation				Close form excitation	
	$\tau_1(ps)$	$\tau_2(ps)$	$\tau_3(ps)$	$\tau_4(ps)$	$\tau_1(ps)$	$\tau_2(ps)$
DTE	0.10(2)	0.20(5)	1.0(2)	55(8)	0.12(8)	6.0(5)
DTE-m5	0.19(1)	0.40(2)	1.3(1)	70(1)	...	...

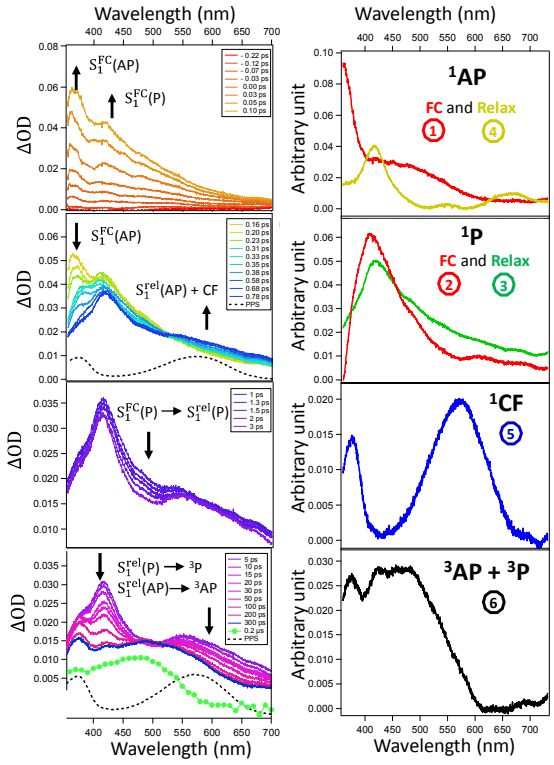

Figure 6. Subpicosecond time-resolved absorption spectra of DTE (left) in chloroform using 320 nm excitation wavelength (All spectra are corrected from the GVD), and spectra (right) of the 6 excited states species of DTE identified by MCR-ALS analysis.

Distinguishing FC states spectral signature from relaxed singlet and triplet states for AP, P and CF species one is a challenging task, because it represents at least 7 species to resolve. We address this issue with the aid of MCR-ALS decomposition (see document S.13 and Figure S.14) of the entire transient data set presented in Figure 6 and following the same strategy we applied in the past for resolving the photophysics of benzophenone[35] and solvatochromic betaine pyridinium.[36] The results of the decomposition, given in the right side panel of Figure 6, consists of six species noticed ① to ⑥ and the associated concentration profils are presented in Figure S.14. As a matter of fact, our purpose is to assign the MCR-ALS spectral features to the photochemical species discussed just above.

As seen on figure S.14, The two first species ① and ②) appear very quickly with a very similar time profile. The species 1 presents a maximum around 360 nm which corroborates the $S_1^{FC}(AP)$ assignment. Similarly, the species ② presents a maximum at 410 nm related by consequence to the P conformer $S_1^{FC}(P)$. After 0.43 ps, two species (③ and ④) appear and decrease over time. These species correspond to the relaxed singlet state of the two conformers. The species ⑤ appears in the beginning and show afterward quasi-constant concentration during the time. This species show spectra with characteristic features of the closed form (CF) and therefore has been attributed to this species. The last species 6 appears continuously and is the last one (with the closed form) still present after 300 ps. As evidence, this species (in black in Figure 6) represent the blend of the triplet conformers.

To the best of our knowledge, we are the first group to present the FC and relaxed singlet states spectra for each conformer of dithienylethene. This is striking to note that FC (②) and relax state spectra (③) are very similar for the P conformer with a maximum near 430 nm. Reversely, two different spectra are obtained for AP conformers comparing ① and ④. In the case of the non-reactive species, a possible explanation is given by the analysis the calculated optimized geometry of the P conformer in the S_1 state which presents a similar geometry as compare to the FC one and which probably induces similar FC factors during $S_1 \rightarrow S_n$ transitions. For the AP conformer, we were not able to find the optimized S_1 state due to wave function instabilities in the S_1(relax) region that is much far from the FC region. We however have to keep in mind that such results can be due to the "scale ambiguity" encountered during MCR-ALS decomposition (see supporting information)

Photoreversion process: spectral signatures revealed.

To complete the study of DTE, transient absorption spectra have been recorded for a blue solution of CF of DTE (in chloroform) following 600 nm laser excitation which corresponds to S_1 excitation (see TD-DFT results above). The data are presented in Figure 7 and the proposed mechanism in Figure 8. Note that the laser perturbation, situated right in the middle of the detection region, (and despite the use of a notch filter), was important in such a way that we just present a restricted spectral region between 400 to 560 nm. Only two temporal windows are necessary to describe the data. First, between 0 and 0.4 ps, an ESA band is rising and slowly shifting around 420 nm together with the formation of a negative band due to bleaching of the ground state. Then between 0.6 and 100 ps a double exponential decay is found with 120 fs and 6 ps characteristic times (Table 3) in total accordance with the data reported by Cassandra *et al.*[37] For shorter times (until ~2 ps), one can notice the decay of ESA band without recovering of ground state (bleaching band is constant); then the ESA band decay continues concomitantly with ground state recovery. The interpretation is straightforward because only a two-steps mechanism is required. First, one observes a decay of FC state toward relaxed state within 120 fs characteristic time $S_1^{FC}(CF) \rightarrow S_1^{rel}(CF)$ followed by an IC toward CF ground state within 6 ps, i.e. $S_1^{rel}(CF) \rightarrow S_0(CF)$. In parallel to this main process, a small part of the electronic population within $S_1^{rel}(AP)$ evolves toward a S_1/S_2 conical intersection in order the photoreversion reaction to proceed within 6 ps characteristic time. Note that we do not succeed to detect the triplet CF species which probably confirms the hypothesis of the adiabatic pathway stipulated before. Finally, as a new result, we publish here, for the first time, the two spectral signatures of both FC and relaxed singlet states of CF.

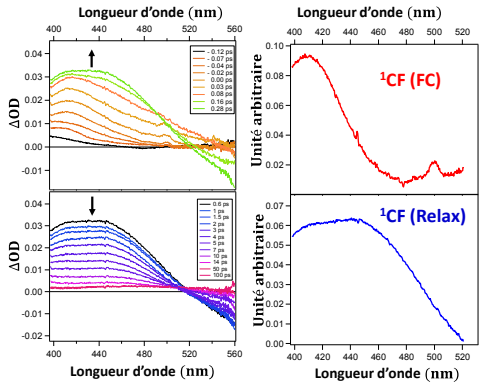

Figure 7. Subpicosecond time-resolved absorption spectra (left) of DTE in chloroform using 600 nm excitation wavelengths (all spectra are corrected from the GVD) and spectroscopic evolution (right) of the two excited states species of DTE identified by MCR-ALS analysis.

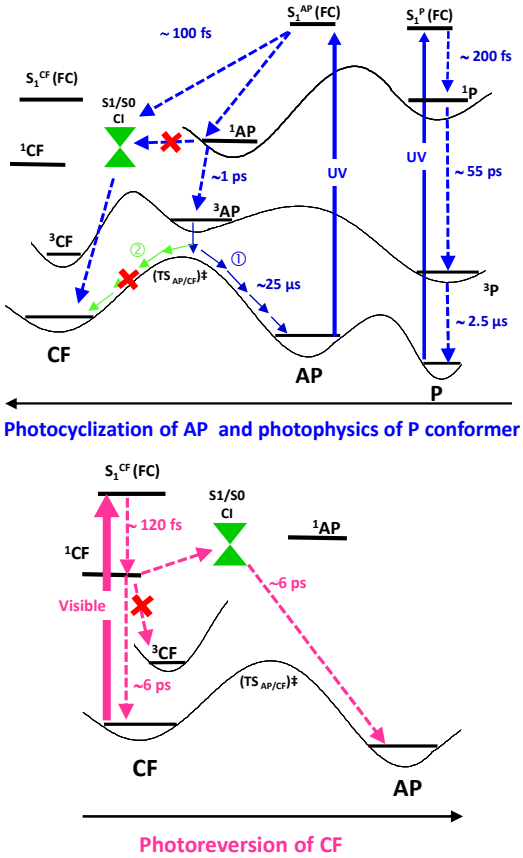

Figure 8. Possible photophysical scheme for a) the photocyclization of DTE and b) the photoreversion of the DTE CF

CONCLUSION

Both photocyclization and photoreversion processes of DTE and the novel bridged analog DTE-m5 have been investigated by state-of-the-art TD-DFT calculations and ultrafast spectroscopy supported by advanced chemometrics data treatments. The overall findings of this study are schematized in Figure 8. Concerning the photoreversion process, we basically confirm the findings of Cassandra *et.al.*[37] i.e., a first ~120 fs vibrational relaxation from $S_1^{FC}(CF)$ to $S_1^{rel}(CF)$ followed by a 6 ps ring-opening reaction in competition with IC to the ground state. Such a low quantum yield of DTE can be explained by the necessity of the system to relax first toward $S_1^{rel}(CF)$ before reaching the conical intersection.[9] As a new result, based on MCR-ALS decomposition, we reported for the first time two distinct spectra for FC and relaxed singlet species of the closed form. The reinvestigation of photocyclization process has been much fruitful. As evidenced by quite similar spectral signature, the photophysics of excited P conformer is characterized by the fact that all excited states either singlet or triplet are located into a very narrow FC region. Starting from the FC region, the initial vibrational relaxation occurs within 200 fs while subsequent relaxed singlet state gives birth to triplet state with high quantum yield (ϕ~0.4) according to ISC process (competitive IC to ground state is expected although not mentioned in Figure 8). Finally, typical triplet ISC occurs within ~2.5 µs. Of course, the situation is drastically different for the AP conformer. From FC region, the direct ring-closing reaction proceeds immediately within ~100 fs passing through the proper CI. It is worth to compare this ultrafast event in chloroform with the 5 ps value reported in monocrystal [12b] probably, the solid phase constraints avoid the molecule to reach the CI easily, making the process slower. Even if we were not able to locate computationally $S_1^{rel}(AP)$, we succeded to obtain its distinct spectral signature compared to FC one. To the best of our knowledge, we are the first group to report the ISC (~1 ps) and subsequent decay (~25 µs) of the triplet state of AP conformer with a difficult-to-detect spectral signature. Furthermore, we demonstrated with the bridged DTE-m5 analog that applying proper constraint on the triplet geometry bring the state close to reactive topologic point. However, we assess the new photocyclization pathway to be less than 10%. Anyhow, this contribution will bring a new light for the photochromism community who needs photoswitch operating within triplet manifolds[16a] or for new insight concerning the photodegradation of diarylethene via triplet state.[4] Optimizing the new photocyclization pathway changing length and/or chemical nature of the bridge is now under investigation in our laboratories.

Acknowledgements

Chevreul Institute (FR 2638), Ministère de l'Enseignement Supérieur et de la Recherche, Région Nord–Pas de Calais and FEDER are acknowledged for supporting and funding this work. Also, this work was granted access to the HPC resources of CINES and IDRIS under the allocation x2016087623 made by GENCI (Grand Equipement National de Calcul Intensif).

Notes and references

(1) (a) Crano, J. C.; Guglielmetti, R. J. *Organic Photochromic and Thermochromic Compounds: Volume 2: Physicochemical Studies, Biological Applications, and Thermochromism*; Springer Science & Business Media, 1999(b) Feringa, B. L. *Molecular switches*; Wiley Online Library, 2001(c) Dürr, H.; Bouas-Laurent, H. *Photochromism: molecules and systems: molecules and systems*; Gulf Professional Publishing, 2003.

(2) (a) Irie, M. *Chemical Reviews* **2000**, *100*, 1683(b) Joachim, C.; Gimzewski, J. K.; Aviram, A. *Nature* **2000**, *408*, 541(c) Raymo, F. M. *Advanced Materials* **2002**, *14*, 401(d) Balzani, V.; Credi, A.; Venturi, M. *ChemPhysChem* **2003**, *4*, 49.

(3) Irie, M.; Fulcaminato, T.; Matsuda, K.; Kobatake, S. *Chemical Reviews* **2014**, *114*, 12174.

(4) Herder, M.; Schmidt, B. M.; Grubert, L.; Paetzel, M.; Schwarz, J.; Hecht, S. *Journal of the American Chemical Society* **2015**, *137*, 2738.

(5) (a) Uchida, K.; Tsuchida, E.; Aoi, Y.; Nakamura, S.; Irie, M. *Chemistry Letters* **1999**, 63(b) Irie, M. *Chemical Reviews* **2000**, *100*, 1685(c) Morimitsu, K.; Kobatake, S.; Irie, M. *Tetrahedron Letters* **2004**, *45*, 1155.

(6) (a) Fukumoto, S.; Nakashima, T.; Kawai, T. *European Journal of Organic Chemistry* **2011**, 5047(b) Fukumoto, S.; Nakashima, T.; Kawai, T. *Angewandte Chemie-International Edition* **2011**, *50*, 1565(c) Li, W.; Jiao, C.; Li, X.; Xie, Y.; Nakatani, K.; Tian, H.; Zhu, W. *Angewandte Chemie* **2013**, *126*, 4691(d) Li, W.; Jiao, C.; Li, X.; Xie, Y.; Nakatani, K.; Tian,

H.; Zhu, W. *Angewandte Chemie International Edition* **2014**, *53*, 4603.

(7) (a) Ishibashi, Y.; Miyasaka, H.; Kobatake, S.; Irie, M.; Yokoyama, Y. *2007 Pacific Rim Conference on Lasers and Electro-Optics, Vols 1-4* **2007**, 1364(b) Ishibashi, Y.; Mukaida, M.; Falkenstrom, M.; Miyasaka, H.; Kobatake, S.; Irie, M. *Physical Chemistry Chemical Physics* **2009**, *11*, 2640(c) Ishibashi, Y.; Okuno, K.; Ota, C.; Umesato, T.; Katayama, T.; Murakami, M.; Kobatake, S.; Irie, M.; Miyasaka, H. *Photochem Photobiol Sci* **2010**, *9*, 172.

(8) Aloïse, S. p.; Sliwa, M.; Pawlowska, Z.; Réhault, J.; Dubois, J.; Poizat, O.; Buntinx, G.; Perrier, A.; Maurel, F.; Yamaguchi, S. *Journal of the American Chemical Society* **2010**, *132*, 7379.

(9) Aloise, S.; Ruan, Y.; Hamdi, I.; Buntinx, G.; Perrier, A.; Maurel, F.; Jacquemin, D.; Takeshita, M. *Physical Chemistry Chemical Physics* **2014**, *16*, 26762.

(10) (a) Pontecorvo, E.; Ferrante, C.; Elles, C. G.; Scopigno, T. *Journal of Physical Chemistry B* **2014**, *118*, 6915(b) Ishibashi, Y.; Fujiwara, M.; Umesato, T.; Saito, H.; Kobatake, S.; Irie, M.; Miyasaka, H. *Journal of Physical Chemistry C* **2011**, *115*, 4265.

(11) (a) Ishibashi, Y.; Okuno, K.; Ota, C.; Umesato, T.; Katayama, T.; Murakami, M.; Kobatake, S.; Irie, M.; Miyasaka, H. *Photochemical & Photobiological Sciences* **2010**, *9*, 172(b) Tani, K.; Ishibashi, Y.; Miyasaka, H.; Kobatake, S.; Irie, M. *Journal of Physical Chemistry C* **2008**, *112*, 11150(c) Miyasaka, H.; Murakami, M.; Itaya, A.; Guillaumont, D.; Nakamura, S.; Irie, M. *Journal of the American Chemical Society* **2001**, *123*, 753(d) Murakami, M.; Miyasaka, H.; Okada, T.; Kobatake, S.; Irie, M. *Journal of the American Chemical Society* **2004**, *126*, 14764(e) Sumi, T.; Takagi, Y.; Yagi, A.; Morimoto, M.; Irie, M. *Chem. Commun. (Cambridge, U. K.)* **2014**, *50*, 3928.

(12) (a) Jean-Ruel, H.; Cooney, R. R.; Gao, M.; Lu, C.; Kochman, M. A.; Morrison, C. A.; Miller, R. J. D. *Journal of Physical Chemistry A* **2011**, *115*, 13158(b) Jean-Ruel, H.; Gao, M.; Kochman, M. A.; Lu, C.; Liu, L. C.; Cooney, R. R.; Morrison, C. A.; Miller, R. J. D. *Journal of Physical Chemistry B* **2013**, *117*, 15894(c) Ishibashi, Y.; Tani, K.; Miyasaka, H.; Kobatake, S.; Irie, M. *Chemical Physics Letters* **2007**, *437*, 243.

(13) (a) Boggio-Pasqua, M.; Ravaglia, M.; Bearpark, M. J.; Garavelli, M.; Robb, M. A. *Journal of Physical Chemistry A* **2003**, *107*, 11139(b) Perrier, A.; Aloise, S.; Olivucci, M.; Jacquemin, D. *Journal of Physical Chemistry Letters* **2013**, *4*, 2190.

(14) Aloise, S.; Sliwa, M.; Buntinx, G.; Delbaere, S.; Perrier, A.; Maurel, F.; Jacquemin, D.; Takeshita, M. *Physical Chemistry Chemical Physics* **2013**, *15*, 6226.

(15) (a) Nakamura, S.; Uchida, K.; Hatakeyama, M. *Molecules* **2013**, *18*, 5091(b) Nakamura, S.; Kobayashi, T.; Takata, A.; Uchida, K.; Asano, Y.; Murakami, A.; Goldberg, A.; Guillaumont, D.; Yokojima, S.; Kobatake, S.; Irie, M. *Journal of Physical Organic Chemistry* **2007**, *20*, 821(c) Dulic, D.; Kudernac, T.; Puzys, A.; Feringa, B. L.; van Wees, B. J. *Advanced Materials* **2007**, *19*, 2898.

(16) (a) Indelli, M. T.; Carli, S.; Ghirotti, M.; Chiorboli, C.; Ravaglia, M.; Garavelli, M.; Scandola, F. *Journal of the American Chemical Society* **2008**, *130*, 7286(b) Murata, R.; Yago, T.; Wakasa, M. *Bulletin of the Chemical Society of Japan* **2011**, *84*, 1336(c) Murata, R.; Yago, T.; Wakasa, M. *Journal of Physical Chemistry A* **2015**, *119*, 11138.

(17) (a) Jukes, R. T. F.; Adamo, V.; Hartl, F.; Belser, P.; De Cola, L. *Inorganic Chemistry* **2004**, *43*, 2779(b) Fukaminato, T.; Doi, T.; Tanaka, M.; Irie, M. *Journal of Physical Chemistry C* **2009**, *113*, 11623.

(18) Yoshida, M.; Kamata, T.; National Institute of Advanced Industrial Science & Technology, Japan . 2010.

(19) Tachibana, H.; National Institute of Advanced Industrial Science & Technology AIST, Japan . 2012.

(20) Ichikawa, S.; Ogura, K.; Mitsubishi Pencil Company, Limited, Japan . 2015.

(21) (a) Ward, C. L.; Elles, C. G. *Journal of Physical Chemistry A* **2014**, *118*, 10011(b) Ward, C. L.; Elles, C. G. *The journal of physical chemistry. A* **2014**, *118*, 10011.

(22) Valley, D. T.; Hoffman, D. P.; Mathies, R. A. *Physical Chemistry Chemical Physics* **2015**, *17*, 9231.

(23) Irie, M.; Sakemura, K.; Okinaka, M.; Uchida, K. *Journal of Organic Chemistry* **1995**, *60*, 8305.

(24) (a) Ruckebusch, C.; Aloise, S.; Blanchet, L.; Huvenne, J. P.; Buntinx, G. *Chemometrics and Intelligent Laboratory Systems* **2008**, *91*, 17(b) Ruckebusch, C.; Sliwa, M.; Pernot, P.; de Juan, A.; Tauler, R. *Journal of Photochemistry and Photobiology C-Photochemistry Reviews* **2012**, *13*, 1.

(25) Takeshita, M.; Tanaka, C.; Miyazaki, T.; Fukushima, Y.; Nagai, M. *New Journal of Chemistry* **2009**, *33*, 1433.

(26) Buntinx, G.; Poizat, O.; Leygue, N. *Journal of Physical Chemistry* **1995**, *99*, 2343.

(27) Kumar, C. V.; Qin, L.; Das, P. K. *Journal of the Chemical Society-Faraday Transactions Ii* **1984**, *80*, 783.

(28) (a) Buntinx, G.; Naskrecki, R.; Poizat, O. *Journal of Physical Chemistry* **1996**, *100*, 19380(b) Moine, B.; Rehault, J.; Aloise, S.; Micheau, J.-C.; Moustrou, C.; Samat, A.; Poizat, O.; Buntinx, G. *Journal of Physical Chemistry A* **2008**, *112*, 4719.

(29) (a) Nakayama, T.; Amijima, Y.; Ibuki, K.; Hamanoue, K. *Review of Scientific Instruments* **1997**, *68*, 4364(b) Ziolek, M.; Lorenc, M.; Naskrecki, R. *Applied Physics B-Lasers and Optics* **2001**, *72*, 843.

(30) Gaussian 09, R. A., Frisch, M. J.; Trucks, G. W.; Schlegel, H. B.; Scuseria, G. E.; Robb, M. A.; Cheeseman, J. R.; Scalmani, G.; Barone, V.; Mennucci, B.; Petersson, G. A.; Nakatsuji, H.; Caricato, M.; Li, X.; Hratchian, H. P.; Izmaylov, A. F.; Bloino, J.; Zheng, G.; Sonnenberg, J. L.; Hada, M.; Ehara, M.; Toyota, K.; Fukuda, R.; Hasegawa, J.; Ishida, M.; Nakajima, T.; Honda, Y.; Kitao, O.; Nakai, H.; Vreven, T.; Montgomery, Jr., J. A.; Peralta, J. E.; Ogliaro, F.; Bearpark, M.; Heyd, J. J.; Brothers, E.; Kudin, K. N.; Staroverov, V. N.; Kobayashi, R.; Normand, J.; Raghavachari, K.; Rendell, A.; Burant, J. C.; Iyengar, S. S.; Tomasi, J.; Cossi, M.; Rega, N.; Millam, N. J.; Klene, M.; Knox, J. E.; Cross, J. B.; Bakken, V.; Adamo, C.; Jaramillo, J.; Gomperts, R.; Stratmann, R. E.; Yazyev, O.; Austin, A. J.; Cammi, R.; Pomelli, C.; Ochterski, J. W.; Martin, R. L.; Morokuma, K.; Zakrzewski, V. G.; Voth, G. A.; Salvador, P.; Dannenberg, J. J.; Dapprich, S.; Daniels, A. D.;

Farkas, Ö.; Foresman, J. B.; Ortiz, J. V.; Cioslowski, J.; Fox, D. J. Gaussian, Inc., Wallingford CT **2009**.

(31) Tomasi, J.; Mennucci, B.; Cammi, R. *Chemical Reviews* **2005**, *105*, 2999.

(32) Peng, C. Y.; Ayala, P. Y.; Schlegel, H. B.; Frisch, M. J. *Journal of Computational Chemistry* **1996**, *17*, 49.

(33) Lietard, A.; Piani, G.; Poisson, L.; Soep, B.; Mestdagh, J.-M.; Aloise, S.; Perrier, A.; Jacquemin, D.; Takeshita, M. *Physical Chemistry Chemical Physics* **2014**, *16*, 22262.

(34) Hania, P. R.; Pugzlys, A.; Lucas, L. N.; de Jong, J. J. D.; Feringa, B. L.; van Esch, J. H.; Jonkman, H. T.; Duppen, K. *Journal of Physical Chemistry A* **2005**, *109*, 9437.

(35) Aloise, S.; Ruckebusch, C.; Blanchet, L.; Rehault, J.; Buntinx, G.; Huvenne, J. P. *Journal of Physical Chemistry A* **2008**, *112*, 224.

(36) Aloise, S.; Pawlowska, Z.; Ruckebusch, C.; Sliwa, M.; Dubois, J.; Poizat, O.; Buntinx, G.; Perrier, A.; Maurel, F.; Jacques, P.; Malval, J.-P.; Poisson, L.; Piani, G.; Abe, J. *Physical Chemistry Chemical Physics* **2012**, *14*, 1945.

(37) Ward, C. L.; Elles, C. G. *Journal of Physical Chemistry Letters* **2012**, *3*, 2995.